Appl Phys A (2013) 110:735–739
DOI 10.1007/s00339-012-7230-x

Applied Physics A
Materials Science & Processing

Determination of femtosecond ablation thresholds by using laser ablation induced photoacoustics (LAIP)

Daniel J.O. Orzi · Fernando C. Alvira · Gabriel M. Bilmes

Received: 12 October 2011 / Accepted: 13 August 2012 / Published online: 21 September 2012

Abstract Femtosecond laser material processing as micromachining and nanoparticles fabrication require a careful control of the fluences deposited on the samples. In many cases, best results are obtained by using fluences slightly above the Laser Ablation Threshold (LAT), therefore its accurate determination is an important requirement. LAT can be obtained by measuring the intensity of the acoustic signal generated during the ablation process as a function of the laser fluence.

In this work femtosecond laser ablation thresholds of commercially polished stainless steel plates, white high impact polystyrene, frosted glass, antique rag papers and silicon oxynitride thin films were determined by using laser ablation induced photoacoustics (LAIP). Results were compared with similar data previously obtained by using a nanosecond Nd:YAG laser.

1 Introduction

Femtosecond laser ablation methods are increasingly used for studying laser–matter interactions and material processing [1–3]. A wide range of applications include high-precision materials micromachining [4], synthesis of nanoparticles [5, 6], Laser Induced Breakdown Spectroscopy [7–9] and thin-film deposition [10, 11]. For those applications a variety of materials are used. Among them, SiON films and glass are used to make waveguides produced by direct-femtosecond laser writing [12, 13]. Femtosecond laser microstructured steel substrates are employed to generate superhydrophobic surfaces for subsequent silanization [14]. Polystyrene plastics are widely used to make microfluidic devices by femtosecond laser ablation [15]. Laser cleaning with ultrashort pulses is a promising tool in conservation and restoration of heritage objects, particularly documents and historical papers. In most of these applications the fluence deposited on the samples is a key parameter, and the knowledge of the Laser Ablation Threshold (LAT) of the treated materials is essential for improving the efficiency and quality of the procedure. For instance, in many cases the best results are obtained by using fluences slightly above the LAT.

Several approaches have been proposed for LAT determination. One of the first methods used is based on photothermal deflection, by detecting the refractive index gradient changes around the crater formed by the ablation process [16–18]. Another widely used procedure is the measurement of the diameter or depth of the craters produced, assuming a Gaussian beam profile for the laser [19, 20]. There are also methods based on the measurement of the quantity of mass extracted [21] and procedures that use a high-speed framing camera to photograph the movement of the material ejected from the surface [22]. The measurement of photoinduced electricity and the charge of ionized species stemming from the ablation process were also reported for the determination of LAT [23].

Some of the techniques described above require complex and expensive laboratory equipment (quartz crystal balances or high-speed cameras). the others are not in real time and involve several steps. An additional problem is that in many cases the values of the ablation thresholds of a material ob-

D.J.O. Orzi (✉) · F.C. Alvira · G.M. Bilmes
Centro de Investigaciones Ópticas, CONICET La Plata-CIC,
CC 3, CP 1897, Gonnet, Buenos Aires, Argentina
e-mail: dorzi@ciop.unlp.edu.ar
Fax: +54-221-4712771

D.J.O. Orzi · G.M. Bilmes
Facultad de Ingeniería, Universidad Nacional de La Plata,
La Plata, Buenos Aires, Argentina

tained by using different techniques do not coincide and there is a large dispersion between the results.

Laser Ablation Induced Photoacoustics (LAIP) was also used to determine LAT in nanosecond ablation regime [24–26]. By using this technique it has been shown that acoustic detection with a microphone allows to monitoring the ablation process in real time and perform ablation curves in a simpler and cheaper way.

In this work we used Laser Ablation Induced Photoacoustics for the determination of femtosecond laser ablation thresholds of commercially polished stainless steel plates; white high impact polystyrene (HIPS), frosted glass, antique rag papers and silicon oxynitride (SiON) thin films. We compare the obtained results with previous data obtained with nanosecond ablation.

2 Experimental setup

Figure 1 shows the experimental setup used. The ablation laser was a pulsed Ti:Sapphire laser of a micromachining station (120 fs, 1 mJ, 800 nm). The beam was focused on the sample using a 10-cm focal lens. A combined system of a $\lambda/2$ plate and a polarizer was used to change the energy of the laser pulse to produce laser fluences (F) ranging $0 < F < 10$ J/cm^2. The energy was monitored by means of a calibrated beam-splitter and a thermopile detector (407A Spectra Physic). All the experiments were performed at normal atmospheric conditions.

The acoustic signal generated during ablation was detected with an electret microphone and a conventional amplifier, and registered in a digital oscilloscope (Tektronix TDS 3032, 300 MHz; 2.5 Gs/s). The peak-to-peak amplitude of the first oscillation of the acoustic signal was measured [24]. Laser ablation threshold fluence (F_0) has been determined as the abscissa of the linear regression plot (linear region) of the acoustic signal (S) as a function of laser fluence.

The studied samples were: commercially polished stainless steel plates, white high impact polystyrene (HIPS), frosted glass, antique rag papers and silicon oxynitride (SiON) thin films (thickness 700 nm approx.) deposited on silicon.

3 Results

Figure 2 shows a typical ablation curve for stainless steel, in which the peak-to-peak amplitude of the acoustic signal was plotted as a function of the Ti:Sapphire laser fluence (the left scale). In the same figure the previous results obtained with nanosecond pulses by using an Nd:YAG laser of 10 ns pulse width at 1064 nm were also plotted (the right scale). Each point on the plot corresponds to a measurement in a fresh position on the sample.

Table 1 Laser ablation thresholds of the studied materials

Sample	Laser ablation threshold (J/cm^2)	
	Femtosecond	Nanosecond [26]
Stainless Steel	0.15 ± 0.03	0.8 ± 0.2
White HIPS	0.12 ± 0.03	2.6 ± 0.5
Frosted Glass	0.15 ± 0.03	4.2 ± 0.8
Rag Paper	0.17 ± 0.04	$2{,}2 \pm 0.5$
SiON	0.04 ± 0.01	3.0 ± 0.5

As it can be seen in Fig. 2, two main regions can be identified in the ablation plot. The first one, located below the ablation threshold, in which no ablation takes place and no acoustic signal can be detected; and the second region, where the acoustic signal has a linear response with the laser fluence. From Fig. 2 the laser ablation threshold fluence of stainless steel was determined as 0.15 ± 0.03 J/cm^2.

Figures 3, 4 and 5 show ablation curves in the fluence region near the threshold made with the Ti:Sapphire laser (left scale) of HIPS, frosted glass and antique rag paper, respectively. In each figure the previous results obtained with nanosecond pulses by using a Nd:YAG laser of 10 ns pulse width at 1064 nm (right scale) were also plotted. Table 1 summarizes the values obtained for the laser ablation thresholds in each case. The uncertainty of these measurements is around 20 %, mainly due to the uncertainty in the determination of their radiated area.

Figure 6 shows the ablation curve for SiON. In this case three main regions can be identified. The first two are extended to values up to 0.7 J/cm^2 and have the same behavior previously discussed for the other studied samples. Around 0.8 J/cm^2 there is a change in the slope of the ablation curve and again a linear behavior is observed for higher fluences. This can be explained assuming that at a higher fluences the laser interacts not only with the SiON film but also with the Si substrate. This was confirmed by inspection of the craters formed, which are shown as inserts in Fig. 6. As it can be seen, the same behavior was observed in the nanosecond regime. From the extrapolation of the first linear part of the curve a thresholds fluence of 0.04 ± 0.01 J/cm^2 was determined for SiON. The extrapolation of the second linear part of the curve gives a value 0.6 ± 0.1 J/cm^2 which is in agreement with the threshold fluence value for Si determined in the literature [27, 28].

4 Discussion and conclusions

From Table 1 in all the samples femtosecond laser ablation threshold fluences are considerably lower, at least by one order of magnitude, than the nanosecond ones. This result is

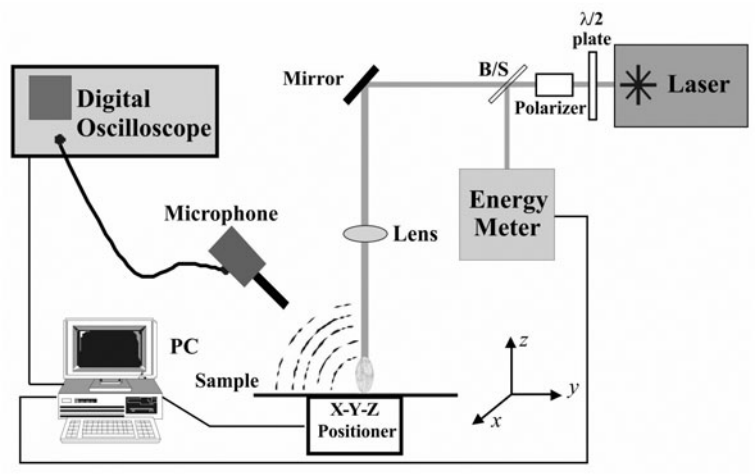

Fig. 1 Experimental setup

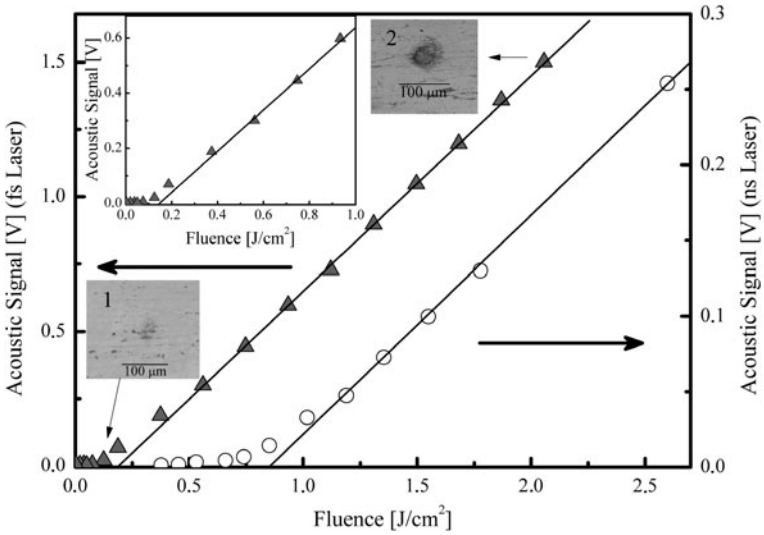

Fig. 2 Femtosecond (*left scale*) and nanosecond (*right scale*) laser ablation curve of stainless steel plate performed with the LAIP technique. The *insert* shows a detail of the low fluence region. Photographs 1 and 2 show the effect of the laser on the substrate. See that only photograph 2 shows a defined crater

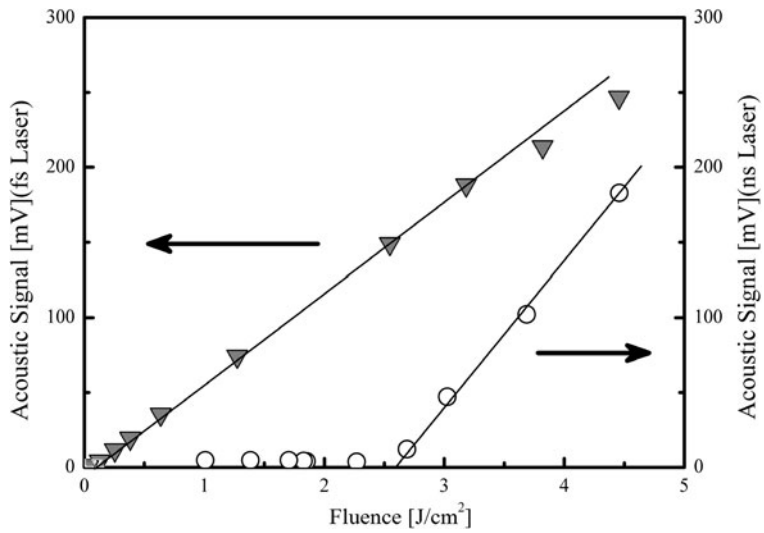

Fig. 3 Femtosecond (*left scale*) and nanosecond (*right scale*) laser ablation curve of white high impact polystyrene performed with the LAIP technique

in agreement with the literature reports [29–31] and can be explained by the different mechanisms that take place during ablation with short and ultrashort laser pulses. In femtosecond regime the time diffusion of heat in the material is several orders of magnitude greater than the pulse duration, therefore the laser interaction is strongly localized. For this

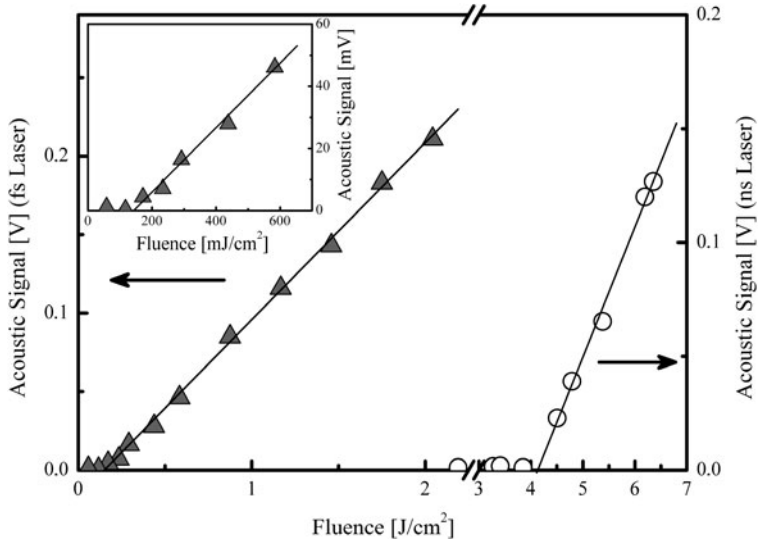

Fig. 4 Femtosecond (*left scale*) and nanosecond (*right scale*) laser ablation curve of frosted glass performed with the LAIP technique

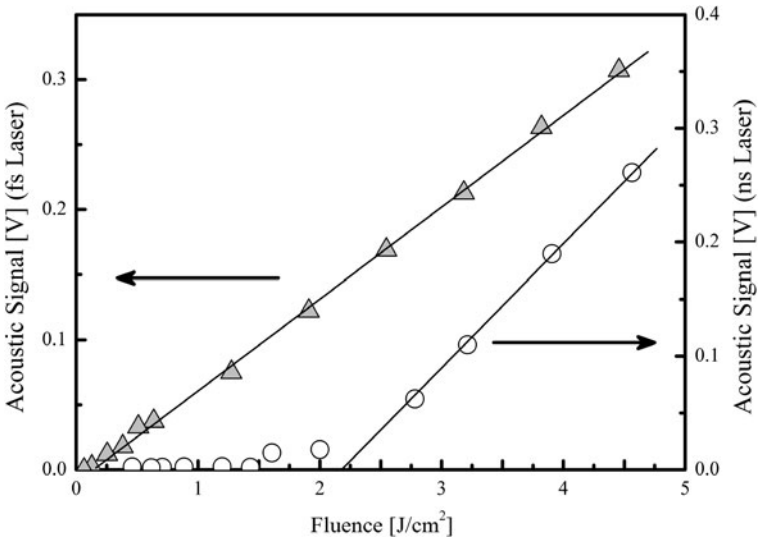

Fig. 5 Femtosecond (*left scale*) and nanosecond (*right scale*) laser ablation curve of antique rag paper performed with the LAIP technique

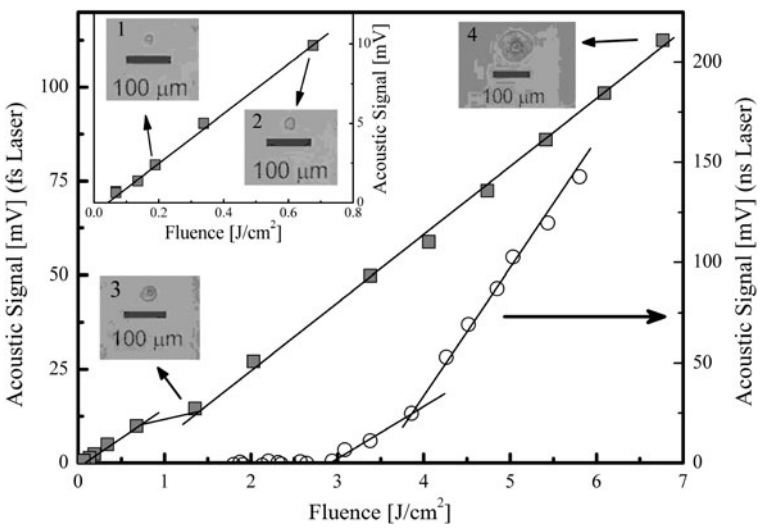

Fig. 6 Femtosecond (*left scale*) and nanosecond (*right scale*) laser ablation curve of SiON thin film deposited on a silicon substrate performed with the LAIP technique. The *insert* shows a detail of the ablation threshold and the first linear region. Photographs 1 to 4 show the craters produced in the SiON film at different fluences. Photographs 1 and 2 show only SiON film ablation. Photographs 3 and 4 show film ablation plus substrate damage

reason the ablation process with femtosecond laser pulses is highly efficient. In the case of laser ablation with nanosecond pulses the first part of the pulse interacts with the sample producing a change of the state from solid to liquid. After that, evaporation from the liquid phase and plasma formation take place. The last part of the laser pulse interacts with this plasma and does not reach the surface of the material [32]. Then, nanosecond laser ablation is less efficient than that performed with femtosecond lasers. For this reason, in regard to nanosecond irradiation, the laser ablation threshold fluence has, in most materials, lower values when femtosecond lasers pulses are used.

In conclusion, by using Laser Ablation Induced Photoacoustics we have measured the femtosecond ablation thresholds of stainless steel, white high impact polystyrene, frosted glass, antique rag paper and SiON films. In the case of SiON, LAIP allows also to detect the fluences in which the laser begins to interact with the substrate. Determination of laser ablation threshold with the LAIP technique has the advantage that is simpler and cheaper than other usually employed methods, and that measurements can be performed in real time.

Acknowledgements The authors wish to thank Dr. Gustavo A. Torchia for fruitful discussions and for providing the SiON samples. This work was partially supported by PICT-Start Up #0999-2010 ANPCyT. DJOO and GMB are researchers from CIC-BA. FCA is a postdoctoral fellow at CONICET.

References

1. C.R. Phipps, *Laser Ablation and Its Applications* (Springer, New York, N.Y., 2007)
2. N.B. Dahotre, *Laser Fabrication and Machining of Materials* (Springer, New York, 2007)
3. J. Perrière, E. Millon, E. Fogarassy, *Recent Advances in Laser Processing of Materials* (Elsevier, Amsterdam, 2006)
4. H. Misawa, S. Juodkazis, *3D Laser Microfabrication: Principles and Applications* (Wiley-VCH, Weinheim, 2006)
5. S. Amoruso, R. Bruzzese, N. Spinelli, R. Velotta, M. Vitiello, X. Wang, G. Ausanio, V. Iannotti, L. Lanotte, Appl. Phys. Lett. **84**(22), 4502–4504 (2004)
6. F.A. Videla, G.A. Torchia, D.C. Schinca, L.B. Scaffardi, P. Moreno, C. Mendez, L.J. Giovanetti, J.M.R. Lopez, L. Roso, J. Appl. Phys. **107**(11) (2010)
7. F.C. Alvira, F.V. Ramirez Rozzi, G.A. Torchia, L. Roso, G.M. Bilmes, J. Anthropol. Sci. **89**, 153–160 (2011)
8. E.L. Gurevich, R. Hergenroder, Appl. Spectrosc. **61**(10), 233A–242A (2007)
9. R.E. Russo, X. Mao, S.S. Mao, Anal. Chem. **74**(3) (2002)
10. A.P. Caricato, A. Luches, Appl. Phys. A, Mater. Sci. Process. **105**(3), 565–582 (2011)
11. M. Cano-Lara, S. Camacho-López, A. Esparza-García, M.A. Camacho-López, Opt. Mater. **33**(11), 1648–1653 (2011)
12. K.M. Davis, K. Miura, N. Sugimoto, K. Hirao, Opt. Lett. **21**(21), 1729–1731 (1996)
13. G.A. Torchia, C. Mendez, I. Arias, L. Roso, J. Piqueras, E. Ruiz, P.L. Pernas, in *Proceedings (IEEE Cat. No. 05EX965)* (IEEE, New York, 2005), pp. 335–337
14. B. Wu, M. Zhou, J. Li, X. Ye, G. Li, L. Cai, Appl. Surf. Sci. **256**(1), 61–66 (2009)
15. R. Suriano, A. Kuznetsov, S.M. Eaton, R. Kiyan, G. Cerullo, R. Osellame, B.N. Chichkov, M. Levi, S. Turri, Appl. Surf. Sci. **257**(14), 6243–6250 (2011)
16. A. Mitra, R.K. Thareja, J. Mater. Sci. **34**(3), 615–619 (1999)
17. J.A. Sell, D.M. Heffelfinger, P. Ventzek, R.M. Gilgenbach, Appl. Phys. Lett. **55**(23), 2435–2437 (1989)
18. J.A. Sell, D.M. Heffelfinger, P.L.G. Ventzek, R.M. Gilgenbach, J. Appl. Phys. **69**(3), 1330–1336 (1991)
19. M. Hashida, A.F. Semerok, O. Gobert, G. Petite, Y. Izawa, J.F. Wagner, Appl. Surf. Sci. **197–198**, 862–867 (2002)
20. S.H. Ko, Y. Choi, D.J. Hwang, C.P. Grigoropoulos, J. Chung, D. Poulikakos, Appl. Phys. Lett. **89**(14) (2006)
21. S. Lazare, V. Granier, J. Appl. Phys. **63**(6), 2110–2115 (1988)
22. Y. Domankevitz, N.S. Nishioka, IEEE J. Quantum Electron. **26**(12), 2276–2278 (1990)
23. D. Vouagner, C. Beleznai, J.P. Girardeau-Montaut, C. Templier, H. Gonnord, Diam. Relat. Mater. **9**(3), 786–791 (2000)
24. G.M. Bilmes, D.J.O. Orzi, O.E. Martínez, A. Lencina, Appl. Phys. B, Lasers Opt. **82**(4), 643–648 (2006)
25. F.C. Alvira, D.J.O. Orzi, G.M. Bilmes, Appl. Spectrosc. **63**(2), 192–198 (2009)
26. D.J.O. Orzi, G.M. Bilmes, in *9th International Conference on Laser Ablation*, Tenerife, Spain (2007)
27. S. Amoruso, C. Altucci, R. Bruzzese, C. De Lisio, N. Spinelli, R. Velotta, M. Vitiello, X. Wang, Appl. Phys. A, Mater. Sci. Process. **79**(4–6), 1377–1380 (2004)
28. A. Cavalleri, K. Sokolowski-Tinten, J. Bialkowski, M. Schreiner, D. von der Linde, J. Appl. Phys. **85**(6), 3301–3309 (1999)
29. E.G. Gamaly, A.V. Rode, B. Luther-Davies, V.T. Tikhonchuk, Phys. Plasmas **9**(3), 949 (2002)
30. M.D. Perry, B.C. Stuart, P.S. Banks, M.D. Feit, V. Yanovsky, A.M. Rubenchik, J. Appl. Phys. **85**(9), 6803–6810 (1999)
31. B.C. Stuart, M.D. Feit, S. Herman, A.M. Rubenchik, B.W. Shore, M.D. Perry, J. Opt. Soc. Am. B, Opt. Phys. **13**(2), 459–468 (1996)
32. L.J. Radziemski, D.A. Cremers, *Laser-Induced Plasmas and Applications* (Marcel Dekker, New York, 1989)